


Atrial fibrosis heterogeneity is a risk for atrial fibrillation in pigs with ischaemic heart failure

Zhihao Zhang^{1,2,3} | Julia Vlcek^{1,3} | Valerie Pauly^{1,2,3} | Nora Hesse^{1,2,3} | Julia Bauer^{1,2,3} | Kavi Raj Chataut^{1,2,3} | Florian Maderspacher^{1,2,3} | Lina Sophie Volz^{1,2,3} | Katharina Buchberger^{1,2,3} | Ruibing Xia^{1,2,3} | Bianca Hildebrand¹ | Stefan Kääh^{1,2,4} | Dominik Schüttler^{1,2,3} | Philipp Tomsits^{1,2,3} | Sebastian Clauss^{1,2,3,4} 

¹Department of Medicine I, Campus Grosshadern, University Hospital Munich, Ludwig-Maximilians University (LMU), Munich, Germany

²German Center for Cardiovascular Research (DZHK), Partner Site Munich, Munich Heart Alliance, Munich, Germany

³Institute of Surgical Research at the Walter-Brendel-Centre of Experimental Medicine, University Hospital, LMU Munich, Munich, Germany

⁴Interfaculty Center for Endocrine and Cardiovascular Disease Network Modelling and Clinical Transfer (ICONLMU), LMU Munich, Munich, Germany

Correspondence

Sebastian Clauss, Department of Medicine I, Campus Grosshadern, University Hospital Munich, Ludwig-Maximilians University (LMU), Marchioninistrasse 15, Munich D-81377, Germany.
Email: sebastian.clauss@med.uni-muenchen.de

Funding information

China Scholarship Council, Grant/Award Number: CSC202006160016; CSC201808130158; Corona-Stiftung, Grant/Award Number: S199/10079/2019; Deutsche Forschungsgemeinschaft, Grant/Award

Abstract

Background: Atrial fibrillation (AF) is the most common arrhythmia and is associated with considerable morbidity and mortality. Ischaemic heart failure (IHF) remains one of the most common causes of AF in clinical practice. However, ischaemia-mediated mechanisms leading to AF are still incompletely understood, and thus, current treatment approaches are limited. To improve our understanding of the pathophysiology, we studied a porcine IHF model.

Methods: In pigs, IHF was induced by balloon occlusion of the left anterior descending artery for 90 min. After 30 days of reperfusion, invasive haemodynamic measurements and electrophysiological studies were performed. Masson trichrome and immunofluorescence staining were conducted to assess interstitial fibrosis and myofibroblast activation in different heart regions.

Results: After 30 days of reperfusion, heart failure with significantly reduced ejection fraction (left anterior oblique 30°, $34.78 \pm 3.29\%$ [IHF] vs. $62.03 \pm 2.36\%$ [control], $p < .001$; anterior-posterior 0°, $29.16 \pm 3.61\%$ vs. $59.54 \pm 1.09\%$, $p < .01$) was observed. These pigs showed a significantly higher susceptibility to AF (33.90% [IHF] vs. 12.98% [control], $p < .05$). Histological assessment revealed aggravated fibrosis in atrial appendages but not in atrial free walls in IHF pigs ($11.13 \pm 1.44\%$ vs. $5.99 \pm .86\%$, $p < .01$ [LAA], $8.28 \pm .56\%$ vs. $6.01 \pm .35\%$, $p < .01$ [RAA]), which was paralleled by enhanced myofibroblast activation ($12.09 \pm .65\%$ vs. $9.00 \pm .94\%$, $p < .05$ [LAA], $14.37 \pm .60\%$ vs. $10.30 \pm 1.41\%$, $p < .05$ [RAA]). Correlation analysis indicated that not fibrosis per se but its cross-regional heterogeneous distribution across the left atrium was associated with AF susceptibility ($r = .6344$, $p < .01$).

Conclusion: Our results suggest that left atrial cross-regional fibrosis difference rather than overall fibrosis level is associated with IHF-related AF susceptibility, presumably by establishing local conduction disturbances and heterogeneity.

Philipp Tomsits and Sebastian Clauss contributed equally to the work and share senior authorship.

This is an open access article under the terms of the [Creative Commons Attribution](https://creativecommons.org/licenses/by/4.0/) License, which permits use, distribution and reproduction in any medium, provided the original work is properly cited.

© 2023 The Authors. *European Journal of Clinical Investigation* published by John Wiley & Sons Ltd on behalf of Stichting European Society for Clinical Investigation Journal Foundation.

Number: MA 2186/14-1; Deutsches Zentrum für Herz-Kreislaufforschung, Grant/Award Number: 81X3600221; 81Z0600206; 81X2600255; European Research Area Network on Cardiovascular Diseases, Grant/Award Number: 01KL1910

KEYWORDS

atrial fibrillation, fibrosis, ischaemic heart failure, left atrial fibrosis, myocardial infarction, pig model, structural remodelling

1 | INTRODUCTION

More than 33 million people worldwide are suffering from atrial fibrillation (AF), the most common sustained cardiac arrhythmia and this number is still increasing by around 5 million new cases per year.¹ AF is associated with numerous complications, most importantly with a fivefold increased risk for stroke,¹ a doubling in dementia risk, a tripling in heart failure risk as well as a doubling in mortality.¹ Current treatment options are limited due to insufficient effectivity or relevant side effects, including proarrhythmic effects, most probably because therapies are not targeting causal mechanisms underlying AF.¹⁻⁴ Since AF pathophysiology is complex and still not fully understood, an improved understanding of AF disease mechanisms is the key to identifying novel targets and developing improved treatment approaches.²⁻⁴

Different mechanistic paradigms summarize our understanding of AF pathophysiology, including the establishment of a vulnerable substrate and enhanced triggered activity as a result of various proarrhythmic remodelling processes.²⁻⁴ Enhanced automaticity or altered calcium homeostasis may lead to focal ectopic firing, whereas action potential shortening or the establishment of conduction barriers by atrial fibrosis result in a vulnerable substrate allowing reentry.²⁻⁴ In around 70% of the patients, AF is thought to be secondary to the underlying heart diseases, most importantly myocardial ischaemia or (ischaemic) heart failure.¹ According to several clinical trials, 6.8%–21% of the patients presenting with an acute myocardial infarction will develop AF.^{5,6}

Previously, we have demonstrated significantly increased left atrial fibrosis in pigs with ischaemic heart failure (IHF) and AF.⁷ However, it remains unclear, whether fibrosis is homogeneously distributed across the atrium and whether the distribution pattern has an impact on AF susceptibility in IHF.

Since pigs are among the most valuable species in electrophysiology research due to their porcine anatomy, haemodynamics and conduction properties, which resemble the human situation quite well, especially when compared to rodent models,^{8,9} we studied the above-mentioned porcine model of IHF to further investigate the ischaemia-mediated proarrhythmic atrial remodelling leading to AF.

2 | MATERIAL AND METHODS

2.1 | Animals

German landrace pigs (age range from 3 to 4 months, average body weight 38.3 ± 2.8 kg) were obtained from *Landwirtschaftliche Forschungsstation Thalhausen*, Technical University of Munich, Kranzberg, Germany, *Moorversuchsgut*, Ludwig-Maximilians-University Munich, Oberschleissheim, Germany and *Lehr- und Versuchsgut der LMU*, Ludwig-Maximilians-University, Munich, Oberschleissheim, Germany. Instrumentation of pigs was conducted in accordance with the 'Guide for the Care and Use of Laboratory Animals' and was approved by the Regierung von Oberbayern (ROB-55.2-2631.Vet_02-10-130 and ROB-55.2-2532.Vet_02-15-209). Twenty-two pigs with IHF and 18 age- and weight-matched control pigs without IHF were included in the study. As animal guidelines evolve and tend to get stricter, it has never been as important to respect the 3R (replacement, reduction and refinement) principle when designing a study. Thus, the current manuscript uses in vivo tracings as well as tissue samples from a previous study,⁷ in addition to new animals. The entire tissue workup is done from first-use tissue samples, and all analyses shown are new and original; none of the data has been published elsewhere.

2.2 | Pig model

Model induction was previously described in detail.^{7,10} In brief, pigs were sedated (by intramuscular ketamine [20 mg/kg], azaperone [10 mg/kg] and atropine [.05 mg/kg]), anaesthetized (induced by intravenous midazolam [.5 mg/kg] and maintained by intravenous fentanyl [.05 mg/kg], propofol [.5 mg/kg/min]) and mechanically ventilated (initial parameters: peak pressure 18–25 mmHg, peep 5 mmHg, tidal volume 6–8 mL/kg, FiO₂ 21%; further adjustments according to regular blood gas test results). The right external jugular vein and right carotid artery were surgically prepared, and sheaths were inserted (9F and 8F, respectively). Myocardial infarction was induced by occlusion of the left anterior descending coronary artery distal to the first diagonal branch for 90 min by a PTCA balloon. The

correct localization of the occlusion was confirmed by angiography. Afterwards, sheaths were removed, the wound was closed and pigs were transferred to the stalls, where they were kept and monitored until the final experiment 30 days later.

2.3 | Invasive haemodynamic measurements

Thirty days after myocardial infarction, invasive haemodynamic measurements were performed as previously described,^{7,10} including left ventricular laevocardiography in two planes (30° left anterior oblique [LAO] and 0° anterior–posterior [AP] projection) as well as measurement of left ventricular systolic and enddiastolic pressure, pulmonary capillary wedge pressure, pulmonary artery pressure, right ventricular pressure and right atrial pressure. All measurements were performed under high right atrial electrical stimulation at 130 bpm (with 1:1 atrioventricular [AV] conduction). Control pigs were assessed in the same fashion but without prior myocardial infarction.

2.4 | Electrocardiography and electrophysiological studies

Electrophysiological studies were performed following a standardized protocol as reported previously.^{7,10} Briefly, a multipolar electrophysiology catheter was placed at the high right atrium to allow atrial stimulation (at 2× pacing threshold). The Wenckebach point was assessed by a progressively decreased pacing cycle length until the atrial signal was no longer conducted 1:1 via the AV node. The effective refractory periods of the atrium and the AV node (AERP and AVERP) were determined by a train of eight fixed stimulations followed by a single premature stimulation at a stepwise decreased pacing cycle length until the premature stimulation failed to induce an atrial signal (AERP) or to propagate to the ventricle via the AV node (AVERP). Six fixed pacing cycle lengths, including 500, 450, 400, 350, 300 and 250 ms, were used to perform ERP measurements. Finally, arrhythmias were induced by rapid burst pacing (at the 2× pacing threshold) at 1200 bpm for 6 s. Per pig, 10 burst pacings were performed. AF was defined as an atrial arrhythmic episode with irregular RR intervals longer than 10 s.

2.5 | Histology

After the electrophysiological study, pigs were euthanized in deep sedation and hearts were removed. Tissue samples

from left and right atrial appendages, atrial free walls and ventricular free walls (remote to the infarct zone) were harvested, fixed in 4% formaldehyde and embedded in paraffin for the following histological staining.

Masson's trichrome staining was performed in paraffin-embedded sections (5 μm) using a Masson-Goldner Trichrome staining kit (Carl Roth GmbH + Co. KG, Germany). After the staining, pictures were acquired at a high-resolution microscope (DM6 B, Leica, Germany) with a 40-fold objective. Ten nonoverlapping pictures per region were analysed by three blinded observers using Adobe Photoshop software. Interstitial fibrosis was assessed by pixel counting using Adobe Photoshop software (the percentage of fibrosis was calculated as the number of interstitial fibrosis pixels [excluding perivascular fibrosis] divided by the total number of pixels per picture). Per pig, 10 nonoverlapping pictures per region were analysed.

Immunofluorescence staining was performed in paraffin-embedded sections (5 μm) by the following steps: The tissue was rehydrated by immersing in xylene, 100% ethanol, 95% ethanol, 70% ethanol and 1× phosphate-buffered saline for 5 min per step. Antigen retrieval was performed at 95°C for 20 min. Then .1% Triton X-100 solution was used for tissue permeabilization, and block buffer (1% goat serum in phosphate-buffered saline) was used to block nonspecific staining for 1 h at room temperature. After blocking, tissue was incubated with anti-α-SMA antibody (Cat#ab150301, Abcam, UK, 1:500) and anti-α-actinin antibody (Cat#A7811, Sigma-Aldrich, USA, 1:200) overnight at 4°C. After washing three times in washing buffer (5% bovine serum albumin +.1% Tween 20 in phosphate-buffered saline) for 5 min, tissue was subsequently incubated with Alexa Fluor™ 488 anti-mouse secondary antibody (Cat#4408S, Cell Signaling Technology, USA, 1:100) and Alexa Fluor™ 647 anti-rabbit secondary antibody (Cat#A21245, Thermo Fisher Scientific, USA, 1:100) for 1 h each. The diluted DAPI solution (Cat#H3570, Thermo Fisher Scientific, USA, 1:1000 in phosphate-buffered saline) was applied to incubate tissue for 10 min following the secondary antibody incubation. After washing three times in phosphate-buffered saline for 5 min, slides were covered by fluorescence mounting medium (Cat#S3023, Dako, Denmark) and sealed by glass coverslips. Immunofluorescence staining pictures were acquired at a high-resolution microscope (DM6 B, Leica, Germany) with a 40-fold objective. Five nonoverlapping pictures per region were taken and analysed by using ImageJ software (National Institutes of Health). The number of α-SMA-positive cells and the total cell number were quantified using the ImageJ counting tool. The percentage of α-SMA-positive cells was calculated by the number of positive cells divided by the total number of cells. Per pig, five nonoverlapping pictures per region were analysed.

2.6 | Statistical analysis

Data are presented as mean \pm SEM. Statistical analysis was performed using GraphPad Prism 9. Differences between two groups were calculated by unpaired *t*-tests. Categorical variables were compared by Fisher's exact test. A significant correlation was identified by the Pearson correlation. A *p*-value of $<.05$ was considered statistically significant.

3 | RESULTS

3.1 | Left anterior descending coronary artery occlusion leads to significant IHF

Myocardial infarction in pigs resulted in a significantly reduced ejection fraction compared to control pigs (LAO 30°, 34.78 \pm 3.29% vs. 62.03 \pm 2.36%, ****p* $<.001$; Figure 1A and AP 0°, 29.16 \pm 3.61% vs. 59.54 \pm 1.09%, ***p* $<.01$; Figure 1B). Consistently, left ventricular enddiastolic pressure (LVEDP, 18.02 \pm 1.16 mmHg vs. 14.11 \pm 1.31 mmHg,

p* $<.05$; Figure 1D), pulmonary capillary wedge pressure (PCWP, 21.34 \pm .97 mmHg vs. 16.40 \pm 1.33 mmHg, *p* $<.01$; Figure 1E) and right atrial pressure (16.30 \pm .85 mmHg vs. 13.40 \pm .79 mmHg, **p* $<.05$; Figure 1H) were significantly increased in IHF pigs compared to control pigs.

There were no differences in left ventricular systolic pressure, pulmonary artery pressure and right ventricular pressure between IHF and control pigs (Figure 1C,F,G, respectively).

3.2 | IHF results in an increased susceptibility for AF without affecting electrical conduction

Pigs with IHF showed a clear arrhythmic phenotype. Compared to control pigs, IHF pigs demonstrated a significantly higher inducibility of AF (33.90% of IHF pigs vs. 12.98% of control pigs, **p* $<.05$; Figure 2A) and a significantly higher percentage of burst pacing attempts resulting in AF (31.72% vs. 15.06%, ****p* $<.001$; Figure 2B). To further investigate electrical conduction properties,

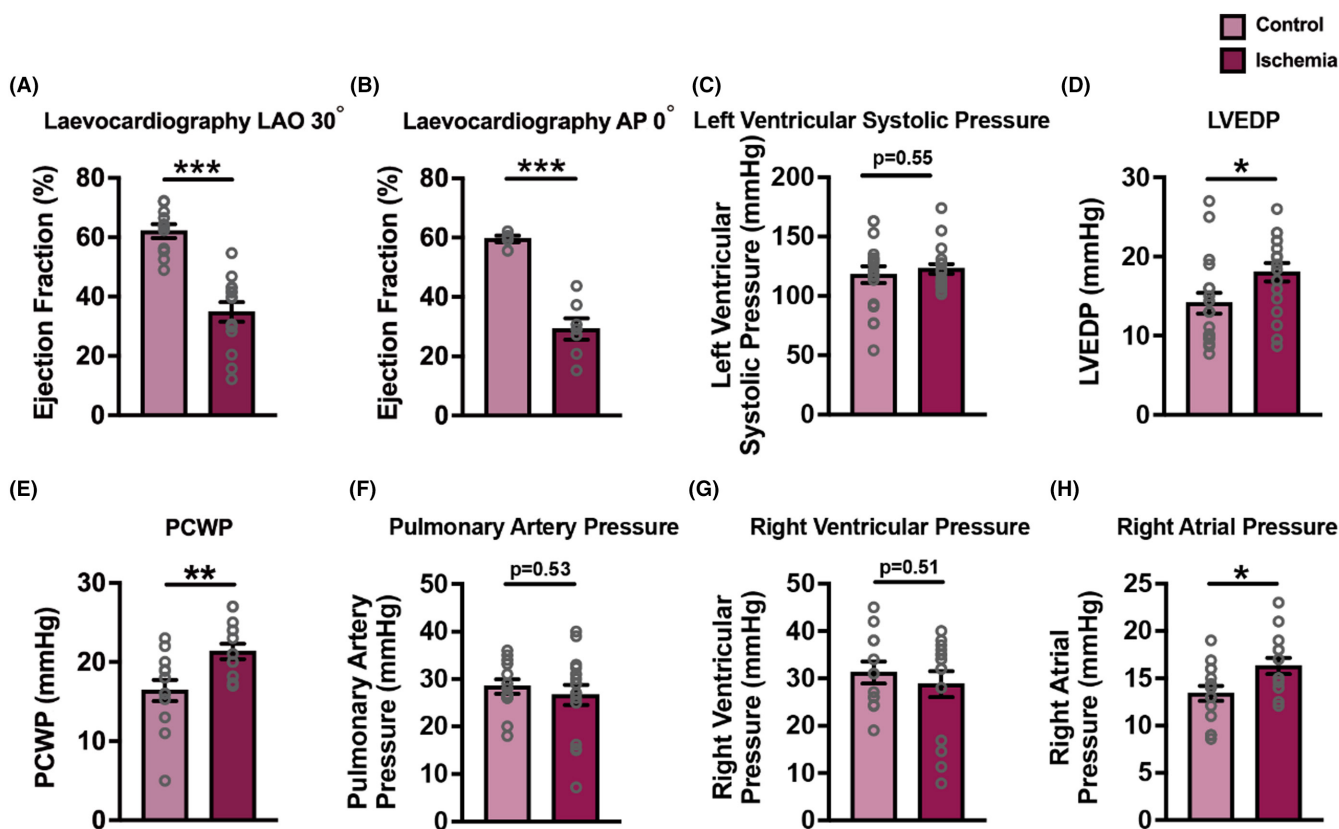


FIGURE 1 Myocardial infarction resulted in significant ischaemic heart failure as observed by haemodynamic measurements. (A) Left ventricular ejection fraction assessed by laevocardiography at left anterior oblique 30° and (B) anterior–posterior 0°; (C) left ventricular systolic pressure; (D) left ventricular enddiastolic pressure (LVEDP); (E) pulmonary capillary wedge pressure (PCWP); (F) pulmonary artery pressure; (G) right ventricular pressure; and (H) right atrial pressure. Bar graphs represent the mean \pm SEM, and grey circles represent the data of individual pigs. Unpaired *t*-tests were applied. **p* $<.05$, ***p* $<.01$, ****p* $<.001$.

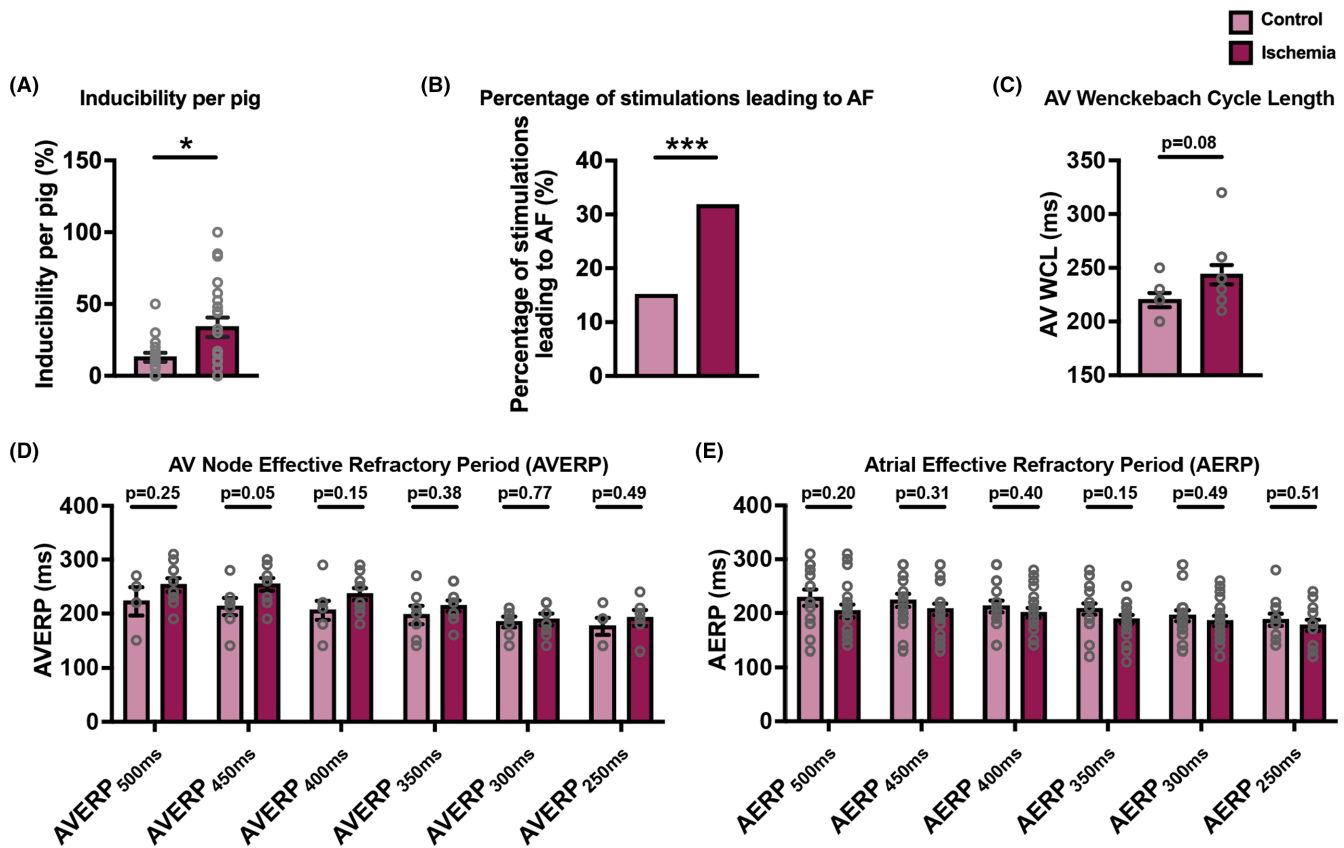


FIGURE 2 Arrhythmia phenotype and electrophysiological properties in control and ischaemic heart failure pigs. (A) Inducibility of atrial fibrillation (AF) per pig; (B) percentage of bursts inducing AF; (C) atrioventricular (AV) Wenckebach cycle length; (D) effective refractory period of the AV node (AVERP); (E) effective refractory period of the atrium (AERP). Bar graphs represent the mean \pm SEM where applicable, and grey circles represent the data of individual pigs. An unpaired *t*-test was applied in (A), (C), (D) and (E), and Fisher's exact test was applied in (B). **p* < .05, ****p* < .001.

invasive electrophysiological studies were performed 30 days after myocardial infarction (IHF pigs) and in age- and weight-matched pigs without myocardial infarction (control pigs). AV Wenckebach cycle length (AV WCL) was prolonged in IHF pigs without reaching statistical significance (243.6 ± 9.0 ms vs. 220.0 ± 6.5 ms, *p* = .08; Figure 2C). Effective refractory periods of the AV node (AVERP, Figure 2D) and the atrium (AERP, Figure 2E) did not differ between groups.

3.3 | IHF results in heterogeneous distribution of interstitial atrial fibrosis

Structural remodelling, especially the development of fibrosis, has been identified as one of the hallmarks of AF pathophysiology. Thus, we quantified interstitial fibrosis in different regions of the heart separately, both in control and IHF pigs. We observed a significant increase of fibrosis in left atrial appendage and right atrial appendage in IHF pigs ($11.13 \pm 1.44\%$ vs. $5.99 \pm .86\%$, ***p* < .01, Figure 3A,B and $8.28 \pm .56\%$ vs. $6.01 \pm .35\%$, ***p* < .01, Figure 3A,E). In

the left atrial free wall (Figure 3A,C), right atrial free wall (Figure 3A,F), left ventricular free wall (Figure 3A,D) and right ventricular free wall (Figure 3A,G), however, the overall level of fibrosis did not significantly differ between control and IHF pigs, demonstrating a heterogeneous distribution of fibrosis in IHF.

3.4 | Aggravated interstitial fibrosis in IHF is paralleled by increased numbers of myofibroblasts in atrial appendages

Activated myofibroblasts are the main source of fibrosis.¹¹ Thus, we quantified myofibroblasts by counting α -SMA-positive cells¹¹ in different regions of the heart, both in control and IHF pigs. We observed a significant increase of myofibroblast numbers only in left atrial appendage and right atrial appendage of IHF pigs ($12.09 \pm .65\%$ vs. $9.00 \pm .94\%$, **p* < .05, Figure 4A,B and $14.37 \pm .60\%$ vs. $10.30 \pm 1.41\%$, **p* < .05, Figure 4A,E), whereas myofibroblast numbers in left atrial free wall (Figure 4A,C), right atrial free wall (Figure 4A,F), left ventricular free wall

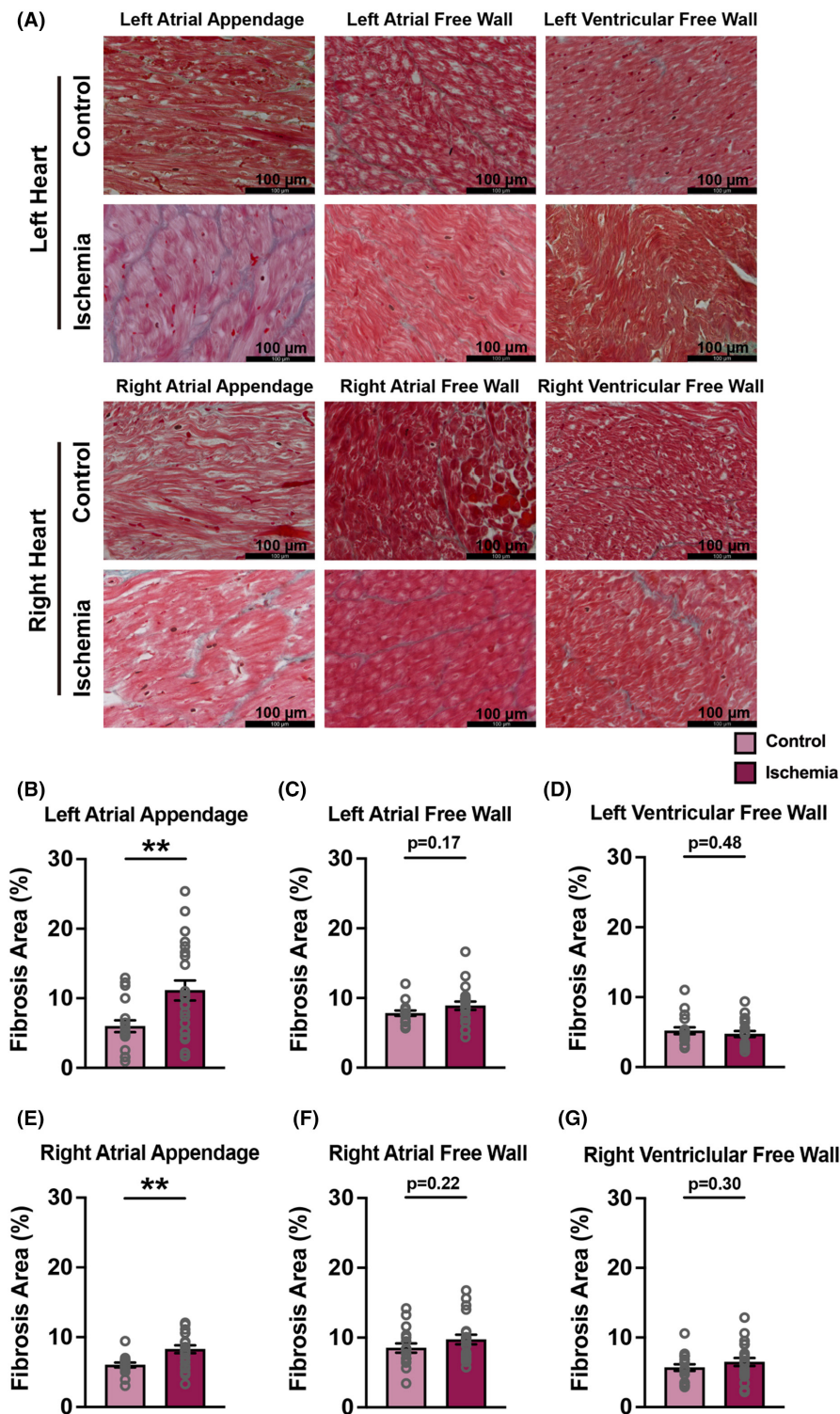


FIGURE 3 Quantification of interstitial fibrosis. (A) Representative images of Masson trichrome-stained tissue slides in control and ischaemic heart failure pigs, quantification of interstitial fibrosis in (B) left atrial appendage, (C) left atrial free wall, (D) left ventricular free wall, (E) right atrial appendage, (F) right atrial free wall and (G) right ventricular free wall. Bar graphs represent the mean \pm SEM, and grey circles represent the data of individual pigs. Unpaired *t*-tests were applied. ***p* < .01.

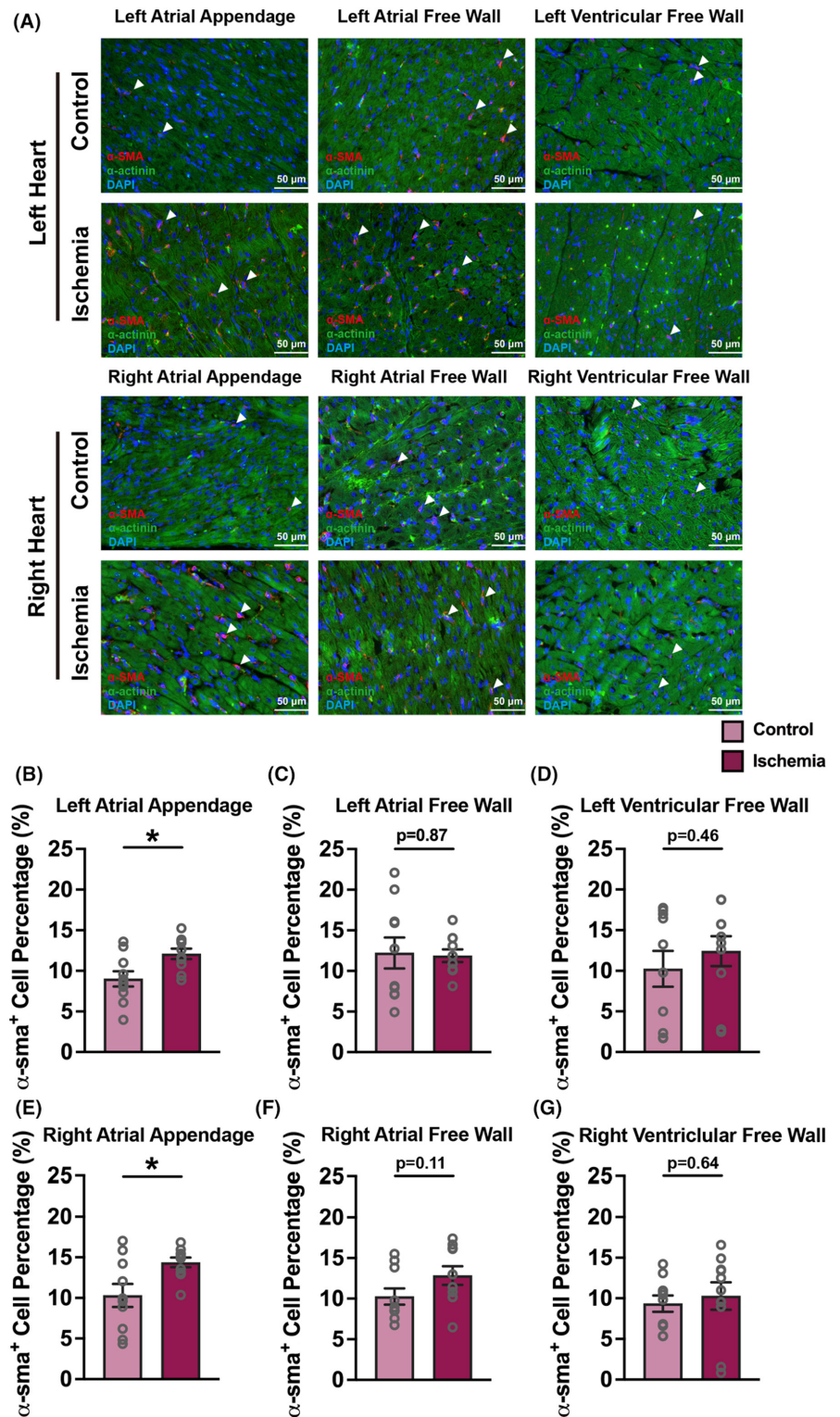
(Figure 4A,D) and right ventricular free wall (Figure 4A,G) did not differ between control and IHF pigs.

3.5 | Left atrial cross-regional fibrosis difference rather than the overall level of fibrosis is associated with AF

Ischaemia resulted in significantly enhanced fibrosis in atrial appendages. However, in pigs with IHF, the

overall level of fibrosis did not correlate with the number of AF episodes in these pigs, neither in atrial appendages (Figure 5A,D) nor in the other regions (Figure 5B,C,E,F). Since we observed that fibrosis was not homogeneously distributed across the atria, we calculated the fibrosis difference between appendages and free walls in both the left and right atria and investigated a potential correlation between fibrosis differences and AF episode numbers. This analysis revealed a significant correlation between fibrosis differences and AF episode numbers in the left

FIGURE 4 Quantification of myofibroblasts. (A) Representative images of immunofluorescence staining in control and ischaemic heart failure pigs; arrowheads indicate myofibroblasts. Quantification of myofibroblasts (α -SMA-positive cell) in (B) left atrial appendage, (C) left atrial free wall, (D) left ventricular free wall, (E) right atrial appendage, (F) right atrial free wall and (G) right ventricular free wall. Bar graphs represent the mean \pm SEM, and grey circles represent the data of individual pigs. Unpaired *t*-tests were applied. * $p < .05$.



atrium ($r = .6344$, ** $p < .01$, Figure 5G), but not in the right atrium of IHF pigs (Figure 5H).

4 | DISCUSSION

Various animal models for AF mimicking different aspects of the disease exist and are highly valuable to

investigate specific underlying mechanisms and to improve our understanding of AF.¹² From a clinical perspective, however, models closely resembling the situation in patients are more relevant, as they may allow direct transfer of novel findings into clinical application, improving patients' health. Thus, we studied an ischaemia model in pigs as (i) myocardial ischaemia is the most common trigger for AF in patients with an incidence of AF

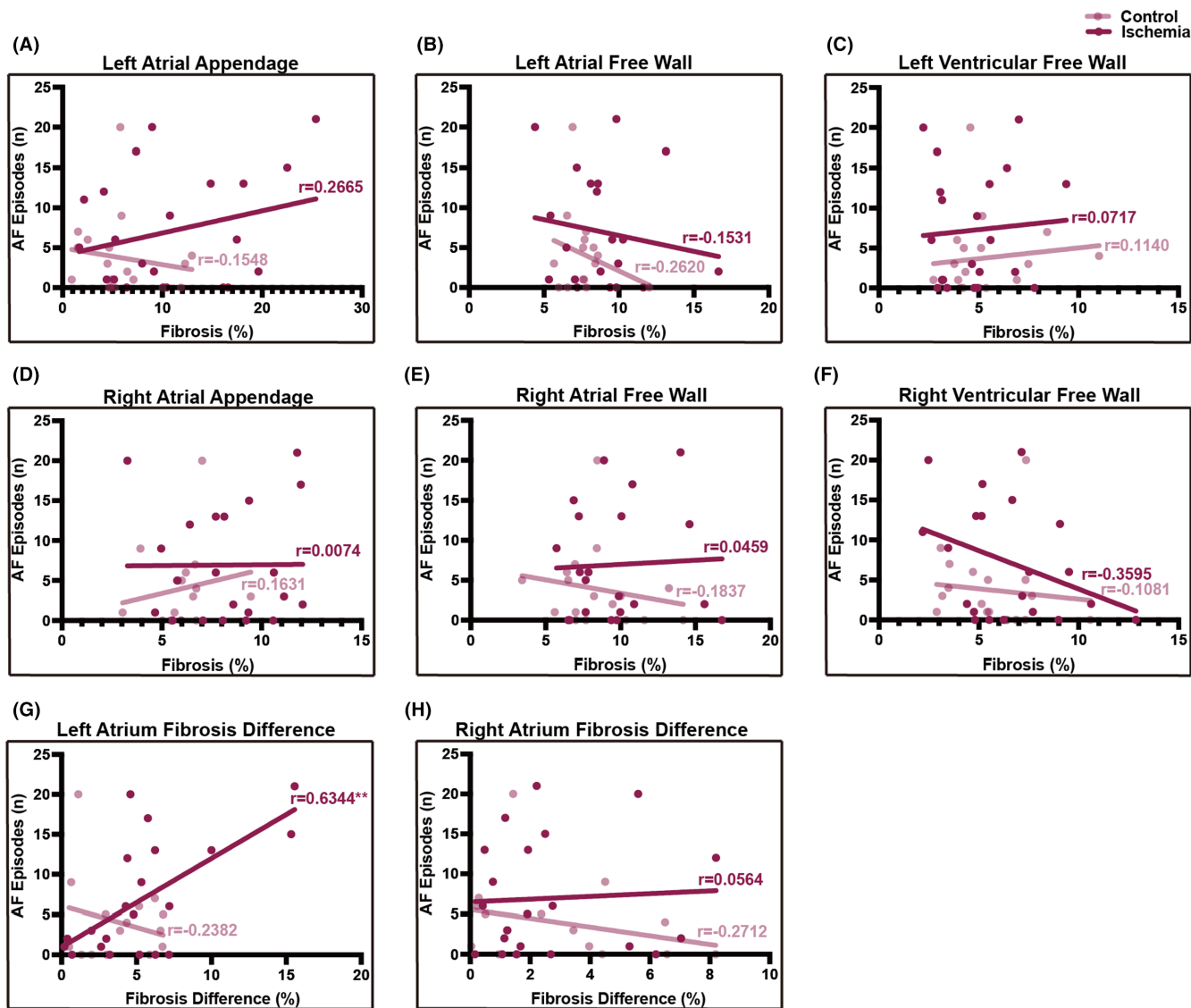


FIGURE 5 Correlation analysis. Correlation of the number of atrial fibrillation episodes with (A) left atrial appendage fibrosis, (B) left atrial free wall fibrosis, (C) left ventricular free wall fibrosis, (D) right atrial appendage fibrosis, (E) right atrial free wall fibrosis, (F) right ventricular free wall fibrosis, (G) left atrium fibrosis difference and (H) right atrium fibrosis difference. Dots represent data of individual pigs. Pearson correlation coefficients were applied. ** $p < .01$.

after myocardial infarction of up to 21%^{1,5,13} and (ii) pigs closely resemble the human anatomy and (electro-)physiology, making pigs an ideal model species for translational AF research.^{8,9} Specifically, the model we used mimics a common clinical situation in patients with ST elevation myocardial infarction that is revascularized 90 min after coronary occlusion, but nevertheless, this short-term ischaemia triggers the development of IHF with subsequent proarrhythmic remodelling, resulting in enhanced vulnerability for AF.^{7,10} As we wanted to investigate ischaemia-mediated proarrhythmic structural remodelling, this preclinical pig model seemed to be well suited.

In our study, we observed a significant and similar to human heart failure phenotype demonstrated by reduced ejection fraction and altered haemodynamics of both the

ventricles (elevated LVEDP) and atria (elevated right atrial and postcapillary wedge pressure, a surrogate for left atrial pressure). We also observed a significantly increased vulnerability to AF in pigs with IHF, which confirms our previous findings in an additional cohort of pigs and justifies using this model to further investigate ischaemia-induced proarrhythmic remodelling.⁷

Next, we explored potential mechanisms underlying this ischaemia-mediated AF susceptibility by in vivo electrophysiology studies and histologic analysis to assess electrical and structural remodelling as two of the major hallmarks of AF pathophysiology.^{2-4,14} Atrial electrophysiological properties, for example AERP, vary in different heart failure models and different animal species.^{8,9} In our IHF pigs, we found no significant alterations

in sinus node function, AV node conduction or atrial effective refractory periods, which is in line with insignificant atrial conduction alterations observed in ischaemic canine hearts previously,¹⁵ suggesting that, 30 days after myocardial infarction, electrical remodelling is not the major driver for enhanced arrhythmogenicity in our model. Myocardial infarction induces necrosis or apoptosis of cardiomyocytes, which are then replaced by reparative fibrosis, establishing a stabilizing scar in the infarct zone. Additionally, ischaemia with progressive heart failure also triggers profibrotic signalling, leading to interstitial fibrosis in other (nonischaemic) areas of the heart including the atria.¹⁶ This results in local conduction heterogeneity, which in turn favours re-entry.^{2-4,14}

In our study, we observed marked regional differences in fibrosis distribution, with significantly increased fibrosis in atrial appendages rather than in atrial free walls and ventricles in IHF pigs. Myofibroblasts have been demonstrated as the main contributor to structural remodelling after heart injury.¹¹ We observed a significantly increased myofibroblast number in atrial appendages but not in atrial free walls and ventricles in IHF pigs. To explore the differences between IHF pigs developing AF and those without AF, we further performed subgroup analyses regarding haemodynamics, electrophysiological measurements, fibrosis amounts and myofibroblast numbers. However, we found no significant differences between groups (data not shown).

Several studies have demonstrated that atrial appendages are an important source of AF.¹⁷ In patients with AF recurrence after ablation, the prevalence of left atrial appendage firing was 27%, with 8.7% of cases being the only source of AF.¹⁷ The BELIFE study also showed that additional electrical left atrial appendage isolation resulted in lower AF recurrence rates compared to extensive ablation of the left atrium alone.¹⁸ In sum, these studies indicate that not only the atria itself but also atrial appendages play an important role in AF.

To further investigate whether the overall degree of fibrosis is important, we evaluated the correlation between fibrosis and the number of AF episodes and could not detect a significant correlation, indicating that the overall level of fibrosis may not be the major determinant of AF, susceptibility in this model. Recently, Ramos and colleagues could similarly demonstrate that in patients with AF the absolute degree of fibrosis is not the key driver for AF.¹⁹ Furthermore, they could show that the heterogeneous distribution of fibrosis within the right atrial appendage does not correlate with altered electrical conduction properties.¹⁹

As interstitial fibrosis has been demonstrated to establish local conduction heterogeneities leading to AF,^{2-4,14} we hypothesized that not only localized but also

cross-regional fibrosis heterogeneity contributes to AF. To address this, we assessed atrial cross-regional differences in fibrosis distribution by subtracting values from appendages and free walls. We could demonstrate that the left atrial fibrosis difference significantly correlates with the number of AF episodes, indicating that not the overall level of atrial fibrosis but rather the left atrial cross-regional fibrosis difference may determine the vulnerability for AF in IHF. Previous studies have indicated that the gross structure and myoarchitecture between the left atrium and the right atrium are markedly different, resulting in differences in electrical conduction as well.²⁰ Thus, left and right atrial remodelling might exert variable effects on AF susceptibility. Compared to the right atrium, the left atrium has been well explored in most previous studies,²¹ and left atrium size has been demonstrated as the strongest independent predictor of new-onset AF in the Framingham study.²² However, we cannot exclude an important role of right atrial remodelling in AF, although we did not find a correlation between right atrial fibrosis differences and AF episode numbers.

Our results demonstrate left atrial cross-regional fibrotic differences in IHF as a potential mechanism for AF in a pig model for the first time. This is in line with previous studies similarly showing the importance of localized fibrosis heterogeneity in AF, for example in the rapid ventricular pacing model in sheep or in the rapid atrial pacing model in dogs.^{8,9} In human end-stage heart failure, nonuniform patchy fibrosis and long fibrotic strands were associated with progressive activation delay, potentially leading to arrhythmias and sudden cardiac death.²³ In a recent study on patients with persistent AF, endomyocardial fibrosis rather than the overall fibrosis has been shown to determine AF complexity.²⁴

As fibrosis is believed to slow conduction and, for example Kazbanov et al. recently demonstrated *in silico* that a larger degree of fibrosis heterogeneity induced more arrhythmias,²⁵ further investigation into this phenomenon could involve visualization of electrical conduction *in vivo*, for example by 3D mapping. Cardiac MRI can be used to anatomically correlate the voltage mapping with cardiac fibrosis and provide further insights into the underlying mechanisms.^{26,27} We believe that a better understanding of the interplay between anatomy/fibrosis and electrical conduction will benefit catheter ablation strategies for AF. Numerous studies indicated that the low effectiveness of AF catheter ablation and impaired atrial function recovery could be linked with interstitial fibrosis across the atrium.²⁸ As pigs share many anatomic and physiological characteristics with humans,⁹ pig models are ideal translational models and can be used to investigate new ablation strategies on the translational road from bench to bedside.

Despite our findings linking left atrial cross-regional fibrosis heterogeneity to AF susceptibility, conclusions with clinical impact should be drawn only with caution. In our pig model, AF episodes were short, self-limiting and induced by burst pacing, probably best representing patients at risk of developing paroxysmal AF. Whether spontaneous AF occurs in this model, that is fully mimicking patients with paroxysmal or persistent AF, needs to be studied, for example by implantable loop recorders in the future.

In sum, we demonstrate that increased AF susceptibility in a porcine IHF model is associated with a heterogeneous distribution of fibrosis across left atrial regions rather than with the overall level of fibrosis. This finding suggests that not fibrosis quantity per se but rather its distribution across the atrium seems to determine AF susceptibility in IHF. Thus, in vivo detection of atrial fibrosis in human patients (e.g. by cardiac MRI or voltage mapping) is important and may help to guide preventive or therapeutic strategies (e.g. specific ablation of the left atrial appendage) in patients at risk to develop AF or patients already suffering from AF, respectively. However, further studies, both in suitable animal models and in human patients, are warranted.

AUTHOR CONTRIBUTIONS

Sebastian Clauss: Supervised the study and designed experiments. Zhihao Zhang, Julia Vlcek, Valerie Pauly, Nora Hesse, Julia Bauer, Kavi Raj Chataut, Florian Maderspacher, Lina Sophie Volz, Katharina Buchberger, Ruibing Xia, Bianca Hildebrand, Dominik Schüttler, Philipp Tomsits and Sebastian Clauss: Performed experiments and analysed results. Sebastian Clauss and Zhihao Zhang: Discussed data and conceived the manuscript. Zhihao Zhang: Prepared the figures. Zhihao Zhang, Philipp Tomsits and Sebastian Clauss: Wrote the manuscript. Sebastian Clauss: Supported and gave suggestions to the study. All authors carefully read and revised the manuscript and agreed to the published version of the manuscript including the authors' names.

ACKNOWLEDGEMENTS

Open Access funding enabled and organized by Projekt DEAL.

FUNDING INFORMATION

This work was supported by the China Scholarship Council (CSC202006160016 to Z.Z., CSC201808130158 to R.X.), the German Research Foundation (DFG; Clinician Scientist Program in Vascular Medicine [PRIME], MA 2186/14-1 to P. T. and D.S.), the German Centre for Cardiovascular Research (DZHK; 81X3600221

to J.B., 81Z0600206 to S.K., 81X2600255 to S.C.), the Corona Foundation (S199/10079/2019 to S. C.) and the ERA-NET on Cardiovascular Diseases (ERA-CVD; 01KL1910 to S.C.). The funders had no role in manuscript preparation.

CONFLICT OF INTEREST STATEMENT

The authors declare no competing interests.

ORCID

Sebastian Clauss  <https://orcid.org/0000-0002-5675-6128>

REFERENCES

- Hindricks G, Potpara T, Dagres N, et al. 2020 ESC guidelines for the diagnosis and management of atrial fibrillation developed in collaboration with the European Association for Cardio-Thoracic Surgery (EACTS): the task force for the diagnosis and management of atrial fibrillation of the European Society of Cardiology (ESC) developed with the special contribution of the European heart rhythm association (EHRA) of the ESC. *Eur Heart J*. 2021;42(5):373-498.
- Brundel B, Ai X, Hills MT, Kuipers MF, Lip GYH, de Groot NMS. Atrial fibrillation. *Nat Rev Dis Primers*. 2022;8(1):21.
- Nattel S, Harada M. Atrial remodeling and atrial fibrillation: recent advances and translational perspectives. *J Am Coll Cardiol*. 2014;63(22):2335-2345.
- Nattel S, Heijman J, Zhou L, Dobrev D. Molecular basis of atrial fibrillation pathophysiology and therapy: a translational perspective. *Circ Res*. 2020;127(1):51-72.
- Schmitt J, Duray G, Gersh BJ, Hohnloser SH. Atrial fibrillation in acute myocardial infarction: a systematic review of the incidence, clinical features and prognostic implications. *Eur Heart J*. 2009;30(9):1038-1045.
- Lubitz SA, Yin X, Rienstra M, et al. Long-term outcomes of secondary atrial fibrillation in the community: the Framingham heart study. *Circulation*. 2015;131(19):1648-1655.
- Clauss S, Schuttler D, Bleyer C, et al. Characterization of a porcine model of atrial arrhythmogenicity in the context of ischaemic heart failure. *PLoS One*. 2020;15(5):e0232374.
- Clauss S, Bleyer C, Schuttler D, et al. Animal models of arrhythmia: classic electrophysiology to genetically modified large animals. *Nat Rev Cardiol*. 2019;16(8):457-475.
- Schuttler D, Bapat A, Kaab S, et al. Animal models of atrial fibrillation. *Circ Res*. 2020;127(1):91-110.
- Schuttler D, Tomsits P, Bleyer C, et al. A practical guide to setting up pig models for cardiovascular catheterization, electrophysiological assessment and heart disease research. *Lab Anim (NY)*. 2022;51(2):46-67.
- Frangogiannis NG. Cardiac fibrosis. *Cardiovasc Res*. 2021;117(6):1450-1488.
- Heijman J, Algalarrondo V, Voigt N, et al. The value of basic research insights into atrial fibrillation mechanisms as a guide to therapeutic innovation: a critical analysis. *Cardiovasc Res*. 2016;109(4):467-479.

13. Jabre P, Jouven X, Adnet F, et al. Atrial fibrillation and death after myocardial infarction: a community study. *Circulation*. 2011;123(19):2094-2100.
14. Clauss S, Sinner MF, Kaab S, Wakili R. The role of MicroRNAs in antiarrhythmic therapy for atrial fibrillation. *Arrhythm Electrophysiol Rev*. 2015;4(3):146-155.
15. Issa ZF, Rosenberger J, Groh WJ, Miller JM, Zipes DP. Ischemic ventricular arrhythmias during heart failure: a canine model to replicate clinical events. *Heart Rhythm*. 2005;2(9):979-983.
16. Hanif W, Alex L, Su Y, et al. Left atrial remodeling, hypertrophy, and fibrosis in mouse models of heart failure. *Cardiovasc Pathol*. 2017;30:27-37.
17. Di Biase L, Burkhardt JD, Mohanty P, et al. Left atrial appendage: an underrecognized trigger site of atrial fibrillation. *Circulation*. 2010;122(2):109-118.
18. Di Biase L, Burkhardt JD, Mohanty P, et al. Left atrial appendage isolation in patients with longstanding persistent AF undergoing catheter ablation: BELIEF trial. *J Am Coll Cardiol*. 2016;68(18):1929-1940.
19. S Ramos K, Pool L, van Schie MS, et al. Degree of fibrosis in human atrial tissue is not the Hallmark driving AF. *Cells*. 2022;11(3):427.
20. Ho SY, Anderson RH, Sanchez-Quintana D. Atrial structure and fibres: morphologic bases of atrial conduction. *Cardiovasc Res*. 2002;54(2):325-336.
21. Chen YC, Voskoboinik A, Gerche A, Marwick TH, McMullen JR. Prevention of pathological atrial remodeling and atrial fibrillation: JACC state-of-the-art review. *J Am Coll Cardiol*. 2021;77(22):2846-2864.
22. Vaziri SM, Larson MG, Benjamin EJ, Levy D. Echocardiographic predictors of nonrheumatic atrial fibrillation. The Framingham Heart study. *Circulation*. 1994;89(2):724-730.
23. Kawara T, Derksen R, de Groot JR, et al. Activation delay after premature stimulation in chronically diseased human myocardium relates to the architecture of interstitial fibrosis. *Circulation*. 2001;104(25):3069-3075.
24. Maesen B, Verheule S, Zeemering S, et al. Endomysial fibrosis, rather than overall connective tissue content, is the main determinant of conduction disturbances in human atrial fibrillation. *Europace*. 2022;24(6):1015-1024.
25. Kazbanov IV, ten Tusscher KH, Panfilov AV. Effects of heterogeneous diffuse fibrosis on arrhythmia dynamics and mechanism. *Sci Rep*. 2016;6:20835.
26. Mewton N, Liu CY, Croisille P, Bluemke D, Lima JA. Assessment of myocardial fibrosis with cardiovascular magnetic resonance. *J Am Coll Cardiol*. 2011;57(8):891-903.
27. Hansen BJ, Zhao J, Fedorov VV. Fibrosis and atrial fibrillation: computerized and optical mapping; a view into the human atria at submillimeter resolution. *JACC Clin Electrophysiol*. 2017;3(6):531-546.
28. Dzeshka MS, Lip GY, Snezhitskiy V, Shantsila E. Cardiac fibrosis in patients with atrial fibrillation: mechanisms and clinical implications. *J Am Coll Cardiol*. 2015;66(8):943-959.

How to cite this article: Zhang Z, Vlcek J, Pauly V, et al. Atrial fibrosis heterogeneity is a risk for atrial fibrillation in pigs with ischaemic heart failure. *Eur J Clin Invest*. 2023;00:e14137. doi:[10.1111/eci.14137](https://doi.org/10.1111/eci.14137)